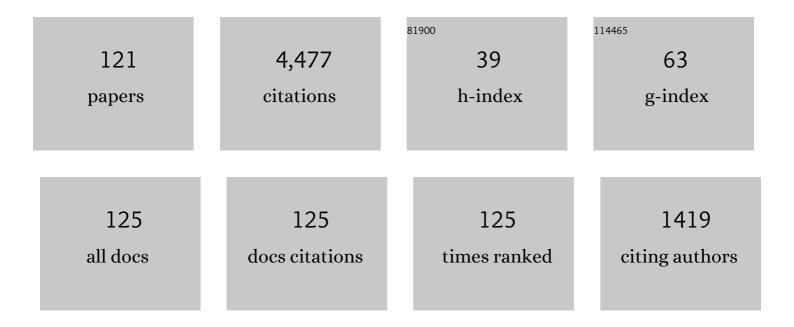
List of Publications by Year in descending order

Source: https://exaly.com/author-pdf/7611740/publications.pdf Version: 2024-02-01



#	Article	IF	CITATIONS
1	Burning plasma achieved in inertial fusion. Nature, 2022, 601, 542-548.	27.8	233
2	Onset of Hydrodynamic Mix in High-Velocity, Highly Compressed Inertial Confinement Fusion Implosions. Physical Review Letters, 2013, 111, 085004.	7.8	215
3	Fusion Energy Output Greater than the Kinetic Energy of an Imploding Shell at the National Ignition Facility. Physical Review Letters, 2018, 120, 245003.	7.8	205
4	The high-foot implosion campaign on the National Ignition Facility. Physics of Plasmas, 2014, 21, .	1.9	149
5	Inertially confined fusion plasmas dominated by alpha-particle self-heating. Nature Physics, 2016, 12, 800-806.	16.7	144
6	Implosion dynamics measurements at the National Ignition Facility. Physics of Plasmas, 2012, 19, .	1.9	125
7	First High-Convergence Cryogenic Implosion in a Near-Vacuum Hohlraum. Physical Review Letters, 2015, 114, 175001.	7.8	117
8	High-density carbon ablator experiments on the National Ignition Facility. Physics of Plasmas, 2014, 21, .	1.9	116
9	Symmetry control of an indirectly driven high-density-carbon implosion at high convergence and high velocity. Physics of Plasmas, 2017, 24, .	1.9	106
10	Demonstration of High Performance in Layered Deuterium-Tritium Capsule Implosions in Uranium Hohlraums at the National Ignition Facility. Physical Review Letters, 2015, 115, 055001.	7.8	101
11	The high velocity, high adiabat, "Bigfoot―campaign and tests of indirect-drive implosion scaling. Physics of Plasmas, 2018, 25, .	1.9	90
12	Design of inertial fusion implosions reaching the burning plasma regime. Nature Physics, 2022, 18, 251-258.	16.7	87
13	High-Performance Indirect-Drive Cryogenic Implosions at High Adiabat on the National Ignition Facility. Physical Review Letters, 2018, 121, 135001.	7.8	86
14	Effect of the mounting membrane on shape in inertial confinement fusion implosions. Physics of Plasmas, 2015, 22, .	1.9	85
15	Dynamic symmetry of indirectly driven inertial confinement fusion capsules on the National Ignition Facility. Physics of Plasmas, 2014, 21, .	1.9	81
16	of Plasmas, 2015, 22, 056318.	1.9	80
17	Exploring the limits of case-to-capsule ratio, pulse length, and picket energy for symmetric hohlraum drive on the National Ignition Facility Laser. Physics of Plasmas, 2018, 25, .	1.9	79
18	Nuclear imaging of the fuel assembly in ignition experiments. Physics of Plasmas, 2013, 20, 056320.	1.9	65

#	Article	IF	CITATIONS
19	Indirect drive ignition at the National Ignition Facility. Plasma Physics and Controlled Fusion, 2017, 59, 014021.	2.1	64
20	Cryogenic tritium-hydrogen-deuterium and deuterium-tritium layer implosions with high density carbon ablators in near-vacuum hohlraums. Physics of Plasmas, 2015, 22, 062703.	1.9	62
21	Development of Improved Radiation Drive Environment for High Foot Implosions at the National Ignition Facility. Physical Review Letters, 2016, 117, 225002.	7.8	61
22	Measurements of an Ablator-Gas Atomic Mix in Indirectly Driven Implosions at the National Ignition Facility. Physical Review Letters, 2014, 112, 025002.	7.8	60
23	Measuring x-ray burn history with the Streaked Polar Instrumentation for Diagnosing Energetic Radiation (SPIDER) at the National Ignition Facility (NIF). Proceedings of SPIE, 2012, , .	0.8	59
24	Hohlraum energetics scaling to 520 TW on the National Ignition Facility. Physics of Plasmas, 2013, 20, .	1.9	59
25	Improved Performance of High Areal Density Indirect Drive Implosions at the National Ignition Facility using a Four-Shock Adiabat Shaped Drive. Physical Review Letters, 2015, 115, 105001.	7.8	58
26	Thin Shell, High Velocity Inertial Confinement Fusion Implosions on the National Ignition Facility. Physical Review Letters, 2015, 114, 145004.	7.8	56
27	X-ray driven implosions at ignition relevant velocities on the National Ignition Facility. Physics of Plasmas, 2013, 20, .	1.9	54
28	Toward a burning plasma state using diamond ablator inertially confined fusion (ICF) implosions on the National Ignition Facility (NIF). Plasma Physics and Controlled Fusion, 2019, 61, 014023.	2.1	53
29	The near vacuum hohlraum campaign at the NIF: A new approach. Physics of Plasmas, 2016, 23, .	1.9	51
30	Hotspot conditions achieved in inertial confinement fusion experiments on the National Ignition Facility. Physics of Plasmas, 2020, 27, .	1.9	50
31	2015, 22, 056314.	1.9	49
32	The role of hot spot mix in the low-foot and high-foot implosions on the NIF. Physics of Plasmas, 2017, 24, .	1.9	49
33	Performance of High-Convergence, Layered DT Implosions with Extended-Duration Pulses at the National Ignition Facility. Physical Review Letters, 2013, 111, 215001.	7.8	47
34	High-energy (>70 keV) x-ray conversion efficiency measurement on the ARC laser at the National Ignition Facility. Physics of Plasmas, 2017, 24, .	1.9	45
35	Development of the CD Symcap platform to study gas-shell mix in implosions at the National Ignition Facility. Physics of Plasmas, 2014, 21, .	1.9	42
36	Short pulse, high resolution, backlighters for point projection high-energy radiography at the National Ignition Facility. Physics of Plasmas, 2017, 24, .	1.9	42

#	Article	IF	CITATIONS
37	Increasing stagnation pressure and thermonuclear performance of inertial confinement fusion capsules by the introduction of a high-Z dopant. Physics of Plasmas, 2018, 25, .	1.9	42
38	X-ray diffraction at the National Ignition Facility. Review of Scientific Instruments, 2020, 91, 043902.	1.3	42
39	Extracting core shape from x-ray images at the National Ignition Facility. Review of Scientific Instruments, 2012, 83, 10E519.	1.3	39
40	Thermonuclear reactions probed at stellar-coreÂconditions with laser-based inertial-confinementÂfusion. Nature Physics, 2017, 13, 1227-1231.	16.7	38
41	Progress of indirect drive inertial confinement fusion in the United States. Nuclear Fusion, 2019, 59, 112018.	3.5	38
42	First beryllium capsule implosions on the National Ignition Facility. Physics of Plasmas, 2016, 23, 056310.	1.9	37
43	Symmetry control in subscale near-vacuum hohlraums. Physics of Plasmas, 2016, 23, .	1.9	34
44	Comparison of implosion core metrics: A 10 ps dilation X-ray imager vs a 100 ps gated microchannel plate. Review of Scientific Instruments, 2016, 87, 11E311.	1.3	34
45	Symmetry tuning of a near one-dimensional 2-shock platform for code validation at the National Ignition Facility. Physics of Plasmas, 2016, 23, .	1.9	33
46	The effects of convergence ratio on the implosion behavior of DT layered inertial confinement fusion capsules. Physics of Plasmas, 2017, 24, .	1.9	33
47	Experimental study of energy transfer in double shell implosions. Physics of Plasmas, 2019, 26, .	1.9	32
48	Enhanced energy coupling for indirectly driven inertial confinement fusion. Nature Physics, 2019, 15, 138-141.	16.7	32
49	Examining the radiation drive asymmetries present in the high foot series of implosion experiments at the National Ignition Facility. Physics of Plasmas, 2017, 24, .	1.9	31
50	Thermal Temperature Measurements of Inertial Fusion Implosions. Physical Review Letters, 2018, 121, 085001.	7.8	31
51	Review of hydrodynamic instability experiments in inertially confined fusion implosions on National Ignition Facility. Plasma Physics and Controlled Fusion, 2020, 62, 014007.	2.1	31
52	Stimulated backscatter of laser light from BigFoot hohlraums on the National Ignition Facility. Physics of Plasmas, 2019, 26, .	1.9	28
53	Experimental results of radiation-driven, layered deuterium-tritium implosions with adiabat-shaped drives at the National Ignition Facility. Physics of Plasmas, 2016, 23, .	1.9	27
54	Ultra-high (>30%) coupling efficiency designs for demonstrating central hot-spot ignition on the National Ignition Facility using a Frustraum. Physics of Plasmas, 2019, 26, .	1.9	25

#	Article	IF	CITATIONS
55	Hotspot parameter scaling with velocity and yield for high-adiabat layered implosions at the National Ignition Facility. Physical Review E, 2020, 102, 023210.	2.1	25
56	In-flight observations of low-mode <i>Ï</i> R asymmetries in NIF implosions. Physics of Plasmas, 2015, 22,	1.9	24
57	Note: A monoenergetic proton backlighter for the National Ignition Facility. Review of Scientific Instruments, 2015, 86, 116104.	1.3	23
58	Visualizing deceleration-phase instabilities in inertial confinement fusion implosions using an "enhanced self-emission―technique at the National Ignition Facility. Physics of Plasmas, 2018, 25, 054502.	1.9	22
59	Hotspot electron temperature from x-ray continuum measurements on the NIF. Review of Scientific Instruments, 2016, 87, 11E534.	1.3	21
60	Mix and hydrodynamic instabilities on NIF. Journal of Instrumentation, 2017, 12, C06001-C06001.	1.2	21
61	Crosstalk in x-ray framing cameras: Effect on voltage, gain, and timing (invited). Review of Scientific Instruments, 2012, 83, 10E135.	1.3	20
62	The effect of shock dynamics on compressibility of ignition-scale National Ignition Facility implosions. Physics of Plasmas, 2014, 21, .	1.9	20
63	Development of an inertial confinement fusion platform to study charged-particle-producing nuclear reactions relevant to nuclear astrophysics. Physics of Plasmas, 2017, 24, .	1.9	20
64	A near one-dimensional indirectly driven implosion at convergence ratio 30. Physics of Plasmas, 2018, 25, .	1.9	20
65	Beryllium capsule implosions at a case-to-capsule ratio of 3.7 on the National Ignition Facility. Physics of Plasmas, 2018, 25, .	1.9	20
66	Achieving 280 Gbar hot spot pressure in DT-layered CH capsule implosions at the National Ignition Facility. Physics of Plasmas, 2020, 27, .	1.9	20
67	Observation of Hydrodynamic Flows in Imploding Fusion Plasmas on the National Ignition Facility. Physical Review Letters, 2021, 127, 125001.	7.8	20
68	Application of cross-beam energy transfer to control drive symmetry in ICF implosions in low gas fill <i>Hohlraums</i> at the National Ignition Facility. Physics of Plasmas, 2020, 27, .	1.9	18
69	Radiative shocks produced from spherical cryogenic implosions at the National Ignition Facility. Physics of Plasmas, 2013, 20, 056315.	1.9	17
70	First demonstration of improved capsule implosions by reducing radiation preheat in uranium vs gold hohlraums. Physics of Plasmas, 2018, 25, .	1.9	17
71	Variable convergence liquid layer implosions on the National Ignition Facility. Physics of Plasmas, 2018, 25, .	1.9	15
72	Development of new platforms for hydrodynamic instability and asymmetry measurements in deceleration phase of indirectly driven implosions on NIF. Physics of Plasmas, 2018, 25, 082705.	1.9	15

#	Article	IF	CITATIONS
73	Performance of beryllium targets with full-scale capsules in low-fill 6.72-mm hohlraums on the National Ignition Facility. Physics of Plasmas, 2017, 24, .	1.9	14
74	Long-duration planar direct-drive hydrodynamics experiments on the NIF. Plasma Physics and Controlled Fusion, 2018, 60, 014012.	2.1	14
75	Maintaining low-mode symmetry control with extended pulse shapes for lower-adiabat Bigfoot implosions on the National Ignition Facility. Physics of Plasmas, 2019, 26, .	1.9	14
76	Methods for characterizing x-ray detectors for use at the National Ignition Facility. Review of Scientific Instruments, 2012, 83, 10E118.	1.3	13
77	Reconstruction of 2D x-ray radiographs at the National Ignition Facility using pinhole tomography (invited). Review of Scientific Instruments, 2014, 85, 11E503.	1.3	13
78	Development of a krypton-doped gas symmetry capsule platform for x-ray spectroscopy of implosion cores on the NIF. Review of Scientific Instruments, 2016, 87, 11E327.	1.3	13
79	Simulations of indirectly driven gas-filled capsules at the National Ignition Facility. Physics of Plasmas, 2014, 21, .	1.9	12
80	Pushered single shell implosions for mix and radiation trapping studies using high-Z layers on National Ignition Facility. Physics of Plasmas, 2019, 26, .	1.9	12
81	Deficiencies in compression and yield in x-ray-driven implosions. Physics of Plasmas, 2020, 27, .	1.9	12
82	Optimized continuum x-ray emission from laser-generated plasma. Applied Physics Letters, 2020, 117, .	3.3	12
83	Fill tube dynamics in inertial confinement fusion implosions with high density carbon ablators. Physics of Plasmas, 2020, 27, .	1.9	11
84	Experiments to explore the influence of pulse shaping at the National Ignition Facility. Physics of Plasmas, 2020, 27, 112708.	1.9	11
85	Simplified model of pinhole imaging for quantifying systematic errors in image shape. Applied Optics, 2017, 56, 8719.	1.8	10
86	Optimization of a high-yield, low-areal-density fusion product source at the National Ignition Facility with applications in nucleosynthesis experiments. Physics of Plasmas, 2018, 25, .	1.9	10
87	A comparison of "flat fielding―techniques for x-ray framing cameras. Review of Scientific Instruments, 2016, 87, 11D622.	1.3	10
88	Spatially resolved X-ray emission measurements of the residual velocity during the stagnation phase of inertial confinement fusion implosion experiments. Physics of Plasmas, 2016, 23, 072701.	1.9	8
89	Neutron Time-of-Flight Measurements of Charged-Particle Energy Loss in Inertial Confinement Fusion Plasmas. Physical Review Letters, 2019, 123, 165001.	7.8	8
90	A simulation-based model for understanding the time dependent x-ray drive asymmetries and error bars in indirectly driven implosions on the National Ignition Facility. Physics of Plasmas, 2019, 26, 062703.	1.9	8

#	Article	IF	CITATIONS
91	Optimization of high energy x ray production through laser plasma interaction. High Energy Density Physics, 2019, 31, 13-18.	1.5	8
92	Recent and planned hydrodynamic instability experiments on indirect-drive implosions on the National Ignition Facility. High Energy Density Physics, 2020, 36, 100820.	1.5	8
93	Characterization of the x-ray sensitivity of a streak camera used at the National Ignition Facility (NIF). Proceedings of SPIE, 2013, , .	0.8	7
94	Principal factors in performance of indirect-drive laser fusion experiments. Physics of Plasmas, 2020, 27, .	1.9	7
95	Measurements of enhanced performance in an indirect drive inertial confinement fusion experiment when reducing the contact area of the capsule support. Physics of Plasmas, 2020, 27, .	1.9	7
96	Experimental quantification of the impact of heterogeneous mix on thermonuclear burn. Physics of Plasmas, 2022, 29, .	1.9	7
97	Automated analysis of hot spot X-ray images at the National Ignition Facility. Review of Scientific Instruments, 2016, 87, 11E334.	1.3	6
98	Using a 2-shock 1D platform at NIF to measure the effect of convergence on mix and symmetry. Physics of Plasmas, 2018, 25, 102702.	1.9	6
99	Beryllium implosions at smaller case-to-capsule ratio on NIF. High Energy Density Physics, 2020, 34, 100747.	1.5	6
100	Hot Spot Evolution Measured by High-Resolution X-Ray Spectroscopy at the National Ignition Facility. Physical Review Letters, 2022, 128, 185002.	7.8	6
101	Simulations of symcap and layered NIF experiments with top/bottom laser asymmetry to impose P1 drive on capsules. Journal of Physics: Conference Series, 2016, 717, 012014.	0.4	5
102	Implementing time resolved electron temperature capability at the NIF using a streak camera. Review of Scientific Instruments, 2018, 89, 10K117.	1.3	5
103	Symmetry tuning and high energy coupling for an Al capsule in a Au rugby hohlraum on NIF. Physics of Plasmas, 2020, 27, .	1.9	5
104	X-ray bang-time measurements at the National Ignition Facility using a diamond detector. Review of Scientific Instruments, 2012, 83, 10E105.	1.3	4
105	NIF Rugby High Foot Campaign from the design side. Journal of Physics: Conference Series, 2016, 717, 012035.	0.4	4
106	Long-duration direct drive hydrodynamics experiments on the National Ignition Facility: Platform development and numerical modeling with CHIC. Physics of Plasmas, 2019, 26, 082703.	1.9	4
107	Reaching 30% energy coupling efficiency for a high-density-carbon capsule in a gold rugby hohlraum on NIF. Nuclear Fusion, 2021, 61, 086028.	3.5	4
108	First graded metal pushered single shell capsule implosions on the National Ignition Facility. Physics of Plasmas, 2022, 29, .	1.9	4

#	Article	IF	CITATIONS
109	Hydroscaling indirect-drive implosions on the National Ignition Facility. Physics of Plasmas, 2022, 29, .	1.9	4
110	Diagnosing residual motion via the x-ray self emission from indirectly driven inertial confinement implosions. Review of Scientific Instruments, 2014, 85, 11E605.	1.3	3
111	Hydrodynamic instabilities and mix studies on NIF: predictions, observations, and a path forward. Journal of Physics: Conference Series, 2016, 688, 012090.	0.4	3
112	Long duration x-ray source development for x-ray diffraction at the National Ignition Facility. Review of Scientific Instruments, 2021, 92, 053904.	1.3	3
113	Control of Be capsule low mode implosions symmetry at the National Ignition Facility. Journal of Physics: Conference Series, 2016, 717, 012033.	0.4	2
114	Using multiple x-ray emission images of inertially confined implosions to identify spatial variations and estimate confinement volumes (invited). Review of Scientific Instruments, 2018, 89, 10G105.	1.3	2
115	Upgrade of the gated laser entrance hole imager G-LEH-2 on the National Ignition Facility. Review of Scientific Instruments, 2021, 92, 033506.	1.3	2
116	A dual high-energy radiography platform with 15 μm resolution at the National Ignition Facility. Review of Scientific Instruments, 2021, 92, 043712.	1.3	2
117	Observation of Nonlinear Optical Coupling in the Kiloelectronvolt X-Ray Regime. IEEE Journal of Quantum Electronics, 2012, 48, 754-759.	1.9	1
118	Performance and operational upgrades of x-ray streak camera photocathode assemblies at NIF. , 2014, , .		0
119	Overview of Performance and Progress with Inertially Confined Fusion Implosions on the National Ignition Facility. , 2015, , .		0
120	History of high-intensity interactions: Physics of the power scaling of the 2.9 angstrom Xe(L) X-ray amplifier to the multi-Petawatt level. , 2008, , .		0
121	Long-Duration X-Ray Source Development for X-Ray Diffraction at The National Ignition Facility. , 2021,		0